eprints@whiterose.ac.uk
https://eprints.whiterose.ac.uk/

Article

Understanding Spatial Variability of NO$_2$ in Urban Areas Using Spatial Modelling and Data Fusion Approaches

Said Munir [1,*], **Martin Mayfield [1] and Daniel Coca [2]**

[1] Department of Civil and Structural Engineering, The University of Sheffield, Sheffield S1 3JD, UK; martin.mayfield@sheffield.ac.uk
[2] Department of Automatic Control and Systems Engineering, The University of Sheffield, Sheffield S1 3JD, UK; d.coca@sheffield.ac.uk
[*] Correspondence: smunir2@sheffield.ac.uk; Tel.: +44-7-986-001-328

Abstract: Small-scale spatial variability in NO$_2$ concentrations is analysed with the help of pollution maps. Maps of NO$_2$ estimated by the Airviro dispersion model and land use regression (LUR) model are fused with measured NO$_2$ concentrations from low-cost sensors (LCS), reference sensors and diffusion tubes. In this study, geostatistical universal kriging was employed for fusing (integrating) model estimations with measured NO$_2$ concentrations. The results showed that the data fusion approach was capable of estimating realistic NO$_2$ concentration maps that inherited spatial patterns of the pollutant from the model estimations and adjusted the modelled values using the measured concentrations. Maps produced by the fusion of NO$_2$-LCS with NO$_2$-LUR produced better results, with r-value 0.96 and RMSE 9.09. Data fusion adds value to both measured and estimated concentrations: the measured data are improved by predicting spatiotemporal gaps, whereas the modelled data are improved by constraining them with observed data. Hotspots of NO$_2$ were shown in the city centre, eastern parts of the city towards the motorway (M1) and on some major roads. Air quality standards were exceeded at several locations in Sheffield, where annual mean NO$_2$ levels were higher than 40 μg/m^3. Road traffic was considered to be the dominant emission source of NO$_2$ in Sheffield.

Keywords: nitrogen dioxide; spatial variability; urban air quality; data fusion; dispersion modelling; land use regression; Sheffield

1. Introduction

Poor air quality is one of the growing environmental issues in urban areas. Long-term exposure to air pollution is known to cause various health issues including both chronic and acute respiratory diseases such as asthma, cancer, cardiovascular diseases, hospital admission and mortality [1–3]. Air pollution caused 6.4 million deaths worldwide in 2015, showing the significance of the impact of poor air quality on human health [4]. Both particulates (e.g., PM$_{10}$ and PM$_{2.5}$) and gaseous pollutants have negative impacts on human health; however, among gaseous pollutants, nitrogen dioxide (NO$_2$) is considered the most serious pollutant for human health [3]. Many Air Quality Management Areas (AQMAs) in the UK were declared due the high levels of NO$_2$ exceeding air quality standards set for human health protection [5]. Among the other challenges of air pollution in urban areas is the quantification of small-scale spatial variability, which is controlled by local emission sources, land use features, building density and height and geographical characteristics. To characterise spatial variability in pollutant concentrations, three approaches are used most commonly [6]: GIS-based interpolation methods, dispersion models and land use regression (LUR) models.

Interpolation methods are used to interpolate (predict) air pollutant concentrations between various air quality monitoring stations to provide better spatial coverage. One of the basic and probably most widely used approaches for interpolation in geostatistics is kriging. Kriging interpolates air pollutant levels (e.g., NO$_2$ concentrations) between two

points by modelling them with Gaussian processes. However, when these approaches are applied at a local scale, such as an intra-city scale, these methodologies are known to produce considerable variations in air pollutant concentrations within a small area and are more effective at large scales, such as national or regional scale [6,7]. For handling these shortcomings, more advanced kriging techniques (e.g., cokriging and universal kriging) can be used to combine modelled and measured values of NO_2, which further improve the performance of the interpolation [8,9]. The second approach for spatial modelling is dispersion modelling techniques, which are probably the most advanced modelling techniques for determining the spatial variability of air pollutants in urban areas. Dispersion models use emission data of different sources (e.g., point, line and area sources), the geophysical characteristics of the study area and meteorological parameters. Dispersion models have the potential to incorporate both temporal and spatial dimensions to complement air pollution monitoring. The third approach for modelling spatial variability is LUR models, which provide an effective alternative to GIS interpolations and dispersion modelling techniques on urban scales. LUR is a spatial modelling approach used most frequently for analysing the spatial variability and quantifying public exposure to air pollution in urban areas. Several authors have preferred LUR to the other approaches [6,10] due the fact that it produces realistic and detailed maps and is easy to apply.

Integrating and merging data and information from several sources is known as data fusion [11]. In the literature, data fusion is also referred to as decision fusion, data combination, data aggregation, multisensor data fusion and sensor fusion. Data fusion techniques merge observed data with modelled data in a mathematical, objective way, adding value to both observed and modelled data. The observed data are improved by filling spatiotemporal gaps, whereas the modelled data are improved by constraining them with observed data [9]. Therefore, data fusion of observed data with modelled data can improve urban-scale air quality mapping. Schneider et al. [9] reported that the accuracy of fused data normally depends on a range of factors, which include (a) the total number of observations, (b) spatial distribution of the network, (c) uncertainty of the measured data, and (d) the ability of the model to accurately predict air pollutant levels with high spatial and temporal resolution.

In this study, firstly, the maps produced by the LUR and Airviro dispersion models are compared for analysing the spatial variability of NO_2 concentrations in Sheffield [12,13]. Secondly, using the universal kriging technique, modelled NO_2 concentrations are fused with the measured concentrations in a view to further improve the spatial maps of NO_2. Measured NO_2 concentrations in the form of points provide absolute values, whereas modelled concentrations provide spatial patterns for the fused high-resolution maps, which are helpful for understanding local-level spatial variability of air pollution and quantifying public exposure in urban areas. This study used measured NO_2 concentrations from three sources (reference sensors, low-cost sensors (LCS) and diffusion tubes) and estimated concentrations from two sources (Airviro dispersion model and LUR model). Measurements of LCS and diffusion tubes are not as reliable as of reference sensors; however, due to cheaper price and maintenance they provide better spatial coverage and a unique opportunity for the spatial modelling of different air pollutants.

The rest of the paper is structured as follows: the methodology of this paper is presented in Section 2. In the Methodology, Section 2.1 provides a brief description of the study area, Section 2.2 describes the air quality monitoring network (AQMN) in Sheffield, Section 2.3 describes the NO_2 map estimated by Airviro, Section 2.4 describes the NO_2 map estimated by LUR and Section 2.5 describes kriging and universal kriging techniques. Results and discussion are presented in Section 3 and the main conclusions of this study are presented in Section 4.

2. Methodology

In this paper, NO_2 concentrations are analysed from the AQMN in Sheffield. In the first part of the paper, spatial variability of NO_2 concentrations ($\mu g/m^3$) is analysed using

three modelling approaches: kriging interpolation, Airviro dispersion model [13] and LUR model [12]. In the second part, NO_2 concentrations measured by various sensors are fused with the NO_2 concentrations estimated by both Airviro and LUR models. For data fusion, one of the geostatistical techniques known as universal kriging is used, which was employed in R programming language using "automap" package [14]. The aim is to develop high-resolution NO_2 maps for understanding the spatial variability of NO_2 in the city of Sheffield, UK.

Below, a brief description of the study area and the AQMN in Sheffield is provided, followed by a description and comparison of the Airviro and LUR NO_2 estimated maps.

2.1. Brief Description of the Study Area

Sheffield (53°23′ N, 1°28′ W) is one of the oldest and most historical cities in South Yorkshire, UK. Sheffield is the second largest city in the Yorkshire and Humber region and had a population of 584,853 in 2019. Sheffield is known as a green city and 61% of its area is composed of green space. The Peak District National Park and Pennine upland range lie to the west of the city and constitute one third of the city's area. Sheffield has a temperate climate. Air pollution is a serious environmental issue in Sheffield and most of the urban area has been declared as an Air Quality Management Area (AQMA) due to the high levels of NO_2 and particulate matter (PM_{10}). Sheffield has a large AQMN, which is briefly described below (Section 2.2).

### 2.2. Air Quality Monitoring Network (AQMN) in Sheffield

There is a large network of one hundred and eighty-eight (188) NO_2 diffusion tubes (DT) in Sheffield (Figure 1a). The Urban Flows Observatory, at the University of Sheffield, has made a network of forty-one (41) low-cost sensors (LCS) which has twenty-eight (28) Envirowatch E-MOTEs and thirteen (13) AQMesh pods, providing continuous hourly data of NO_2 concentrations (Figure 1b). Furthermore, in Sheffield, there are three (3) Automatic Urban and Rural Network (AURN) reference sites run by the UK Department of Environment, Food and Rural Affairs (DEFRA) and five (5) reference stations run by the Sheffield City Council (SCC) (Figure 1b). All these sensors make a multi-layer network providing NO_2 data. In this paper, NO_2 data for over a year (August 2019 to September 2020) are analysed. A summary of the NO_2 data from the network is provided in Table 1. Further details on the network can be found in [12].

Table 1. Summary of annual mean NO_2 concentrations ($\mu g/m^3$) measured by diffusion tubes (DT), automatic urban and rural network (AURN), Sheffield City Council (SCC) and low-cost sensors (LCS) (AQMesh and Envirowatch) in Sheffield (August 2019 to September 2020).

Metrics	DT NO_2	AURN	SCC	AQMesh/Envirowatch E-MOTE
Minimum	13.58	19.09	8.12	12.69
1st Quartile	28.29	21.00	24.05	25.08
Median	33.77	22.90	24.62	34.23
Mean	34.23	24.69	21.53	38.70
3rd Quartile	40.00	27.50	25.02	42.36
Maximum	91.75	32.09	25.86	136.81
Standard Deviation	9.65	6.68	7.53	27.69
Number of Sensors	188	3	5	41
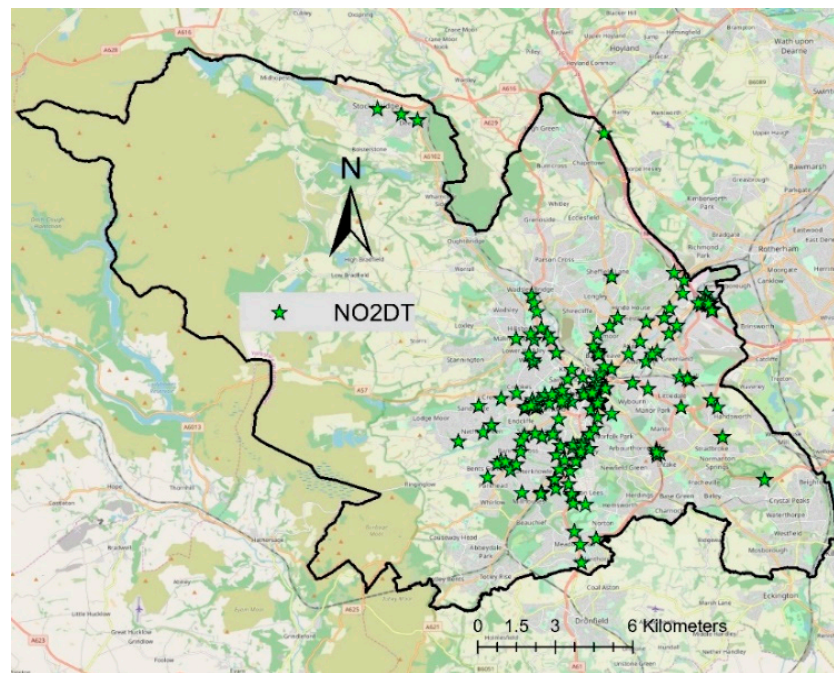
(**a**)
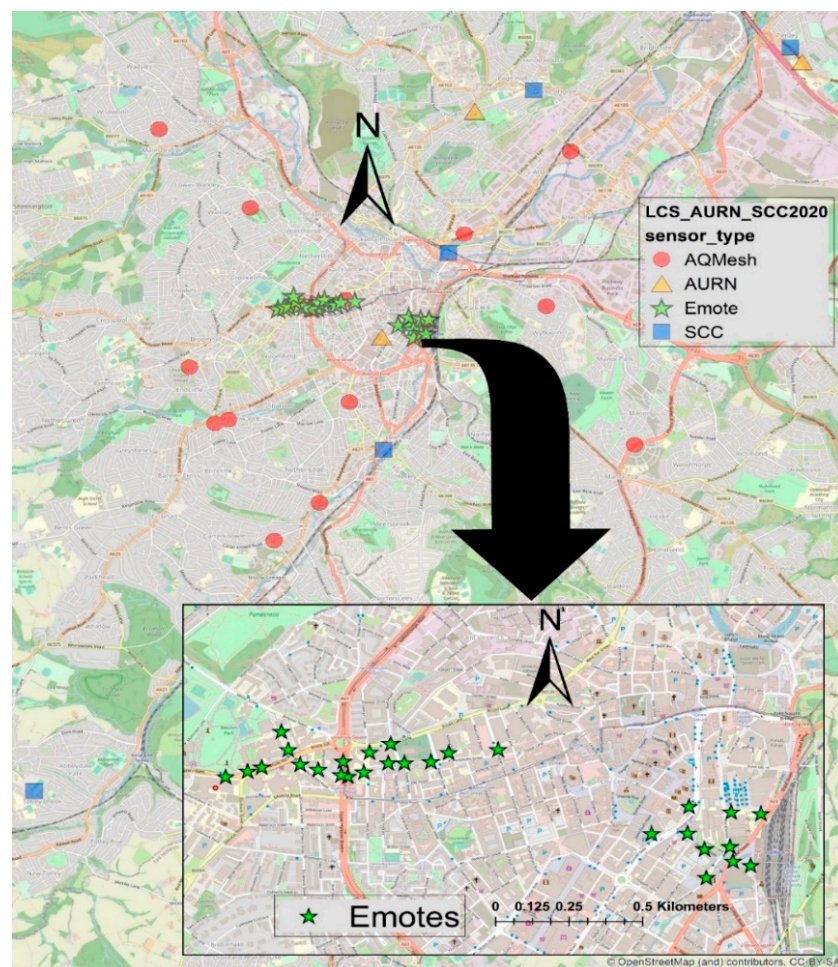
(**b**)

Figure 1. Showing the locations of DT, LCS (both AQMesh pods and Envirowatch E-MOTEs), AURN and SCC monitoring sites in Sheffield: (**a**) DT locations; (**b**) AURN, SCC and LCS locations.

2.3. NO₂ Map Estimated by Airviro

The Airviro dispersion model's estimated map of NO_2 concentrations is adopted from Munir et al. [13], who used the Airviro (version 4.01) dispersion model, which is an integrated modelling system for managing the emission database, modelling the dispersion of pollutants, and handling air quality data. Airviro is a state of the art dispersion model used by many researchers, consultants and local authorities globally for air quality modelling. Like other dispersion models, Airviro requires local topography, pollutant emissions and meteorological data to produce maps of estimated air pollutants. The Airviro model, the required inputs and produced outputs are discussed in detail in Munir et al. [13]. Munir et al. [13] estimated the map of NOx concentrations, which were converted to NO_2 by analysing the ratio of NO_2/NOx. The original map is given in Munir et al. [13] and the adopted map which is further analysed in this paper is shown here in Figure 2. The resulting estimated map showed hotspots of NO_2 concentrations around the city centre and eastern part of the city towards the Tinsley Roundabout (M1 J34S). NO_2 concentrations decrease gradually going away from the city centre, particularly towards the west and northwest of the city.
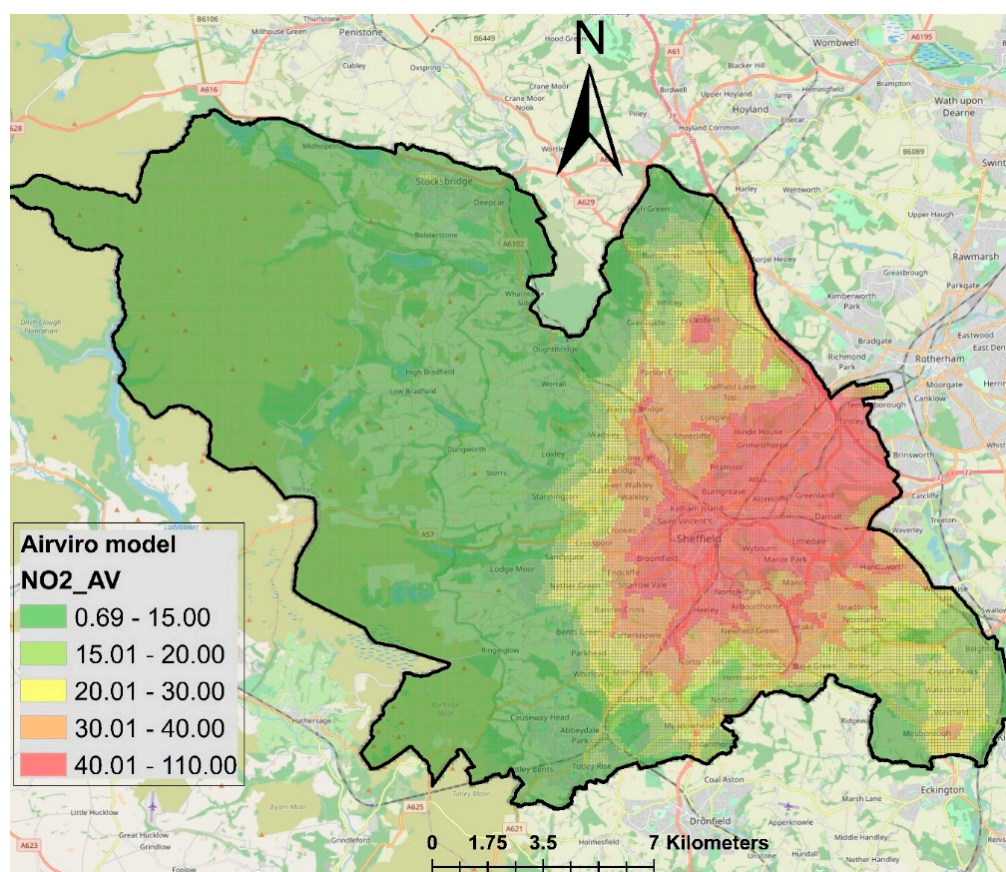

Figure 2. Spatial variability of annual mean modelled NO_2 in Sheffield. Maps were developed using Airviro model (modified from [13]).

2.4. NO₂ Map Estimated by LUR

The LUR map used here is adopted from Munir et al. [12]. LUR is a widely employed approach for the estimation of air pollution exposure using geographical information systems (GIS) and statistical analysis to determine the association between geographical features and measured atmospheric pollutant concentrations [15]. The LUR approach was introduced by Briggs et al. [15] and since then has been used in numerous studies around the world [16–23]. LUR models associate pollutant concentrations, such as NO_2, to site-specific geographical characteristics, e.g., topography, land use, population density and

altitude. The use of these variables in the regression model is known to capture small-scale variability on a city scale [24]. For more details, see [12]. The resulting map produced by the LUR model [12], employing a generalised additive model, a nonlinear regression approach, is shown in Figure 3, which is a high-resolution (100 m × 100 m) map. Figure 3 demonstrates higher levels of NO_2 in the city centre, eastern side of the city and on major roads. As compared to Figure 2, here, the busy roads are successfully highlighted, showing high levels of NO_2 concentrations.
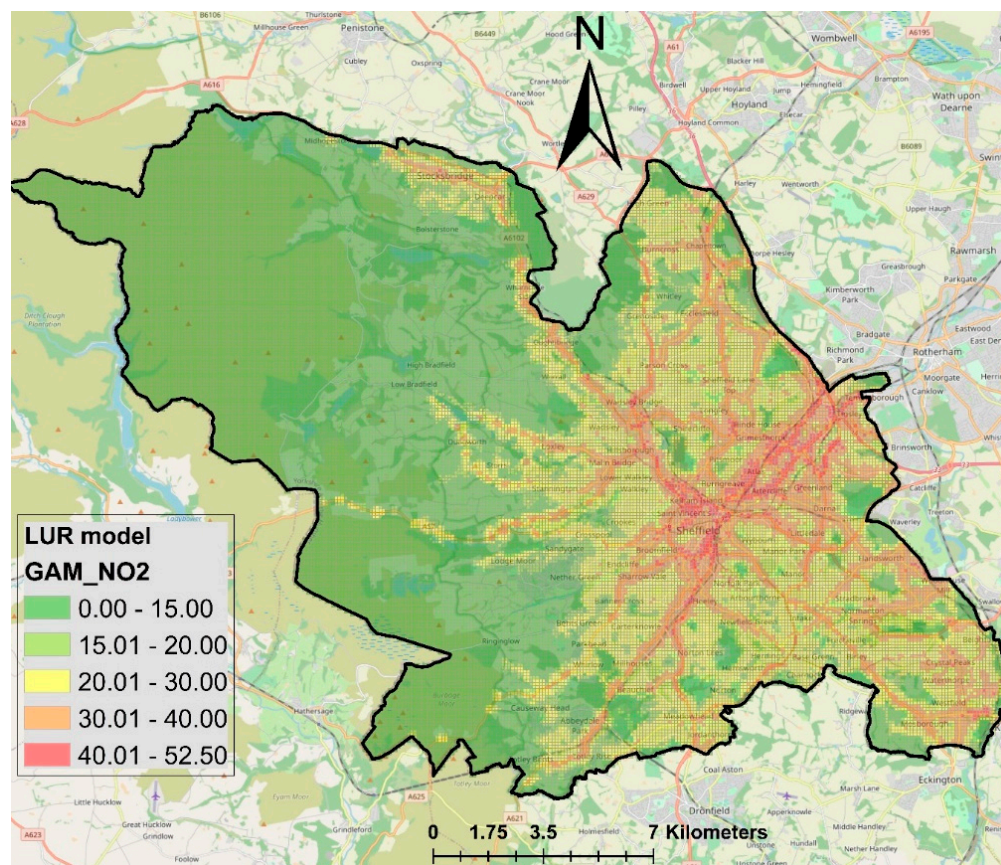

Figure 3. Maps of annual mean modelled NO_2 ($\mu g/m^3$) estimated by LUR model in Sheffield. Modified from [12].

2.5. Kriging and Universal Kriging

Kriging is a type of geostatistical interpolation technique based on statistical models that include statistical relationships among the measured points (autocorrelation). Kriging is a form of probabilistic and local interpolation technique. Kriging uses Gaussian processes for interpolating between various spatial points.

The kriging formula is expressed as:

$$Z_o(S_o) = \sum_{i=1}^{i=n} \lambda i Z i (S i) \tag{1}$$

where $Zi(Si)$ is the measured value at the ith location, λi is an unknown weight for the measured value at the ith location, $Z_o(S_o)$ is the predicted value at the prediction location.

Simple kriging is used for stationary data if the mean is known; otherwise, ordinary kriging is used. To fuse (integrate) model estimations with measured NO_2 concentrations, here, we employed the universal kriging technique, which is more advanced and capable of handling data with more than one correlated variable. In universal kriging, the additional observations of one or more covariates may lead to increased precision of the predictions. This approach enables the merging of NO_2 observations from a network of sensors, with modelled values providing spatial information from the air quality models. Universal krig-

ing, in contrast to ordinary kriging, allows the overall mean to be non-constant throughout the domain and to be a function of one or more explanatory variables [9,25]. Universal kriging is similar to kriging, with external drift and mathematically equivalent to regression kriging or residual kriging [8]. In this paper, measured values are fused with LUR and Airviro estimation using "automap" packages [14] in R programming language [26].

2.6. Model Validation

Performance of the universal kriging technique was assessed by calculating several statistical metrics. Statistical metrics used for comparing measured and estimated concentrations were factor of two (FAC2), mean bias error (MBE), mean absolute error (MAE), root mean square error (RMSE) and correlation coefficient (r). MAE and RMSE show the size of the average error; however, they do not provide information on the relative magnitude of the difference between predicted and observed values as these are based on absolute values of the difference between estimated and measured values. On the other hand, MBE describes the direction of the error bias. A negative value of MBE shows that predicted values are smaller than the observed values, showing underprediction of the model. FAC2 is the percentage of the predictions within a factor of two of the observed values and the correlation coefficient demonstrates the linear relationship between observed and estimated concentrations. For more details on these metrics see Munir et al. [12,13].

For comparison purposes, the measured data collected by different sets of sensors were split into training and testing datasets. Training dataset (75% of the data) and testing dataset (25% of the dataset) were randomly selected using "caTools" package of R programming language. After assessing the model performance, the model was retrained using the whole dataset and applied to the rest of the city where measured data were not available.

3. Results and Discussion

In this section, firstly, the measured and interpolated NO_2 concentrations ($\mu g/m^3$) are analysed (Section 3.1), followed by data fusion (Section 3.2), wherein model estimations are fused with measured NO_2 concentrations.

3.1. Measured and Interpolated NO_2 Concentrations

Figure 4 demonstrates both measured and interpolated NO_2 concentrations for DT. Annual mean of measured NO_2 concentrations ($\mu g/m^3$) ranged from 13.58 to 91.75. It should be noted that the air quality limit for annual mean NO_2 concentrations is 40 ($\mu g/m^3$); therefore, to protect human health, annual mean NO_2 levels should not exceed this level. The observed levels (Figure 4) show that the air quality limits are exceeded at several sites in the city, especially in the city centre and on main roads. These readings are only for point locations and there are large gaps between these locations. To create a continuous map, in this paper, we used ordinary kriging for predicting NO_2 concentrations for the locations where measured concentrations were not available. Interpolated concentrations are shown in Figure 4b, which demonstrates that air quality standards are violated in some parts of the city centre and in the northeast of the city. However, in most of the city centre and northeast of the city, NO_2 levels range from 35 to 40 ($\mu g/m^3$). In the northwest and areas adjacent to the city centre, the NO_2 levels ranged from 30 to 35. Deep green and light green areas mostly in the southwest part of the city show NO_2 levels in the range of 20 to 30 ($\mu g/m^3$), which is the area next to the Peak District National Park.
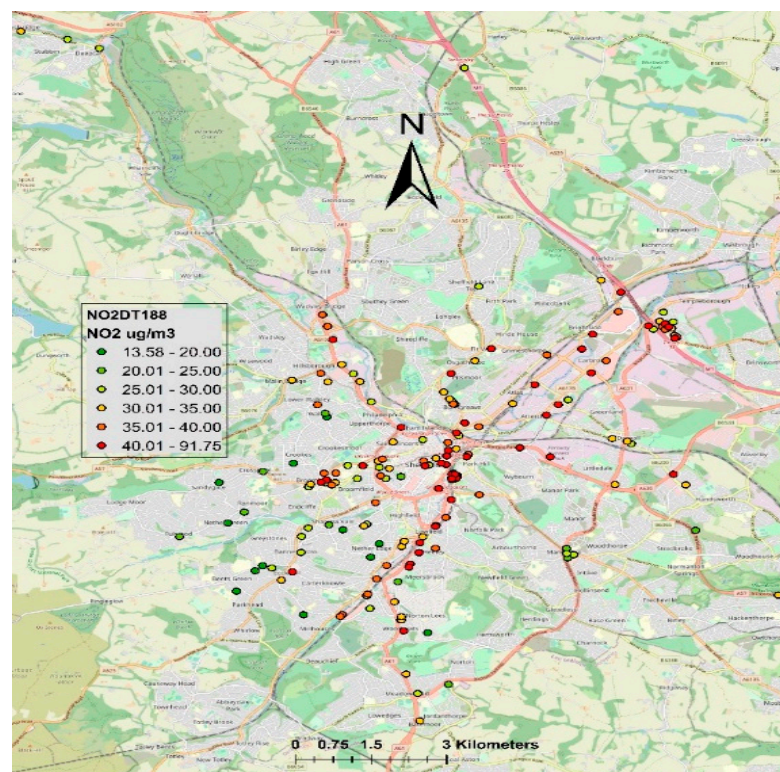
(**a**)
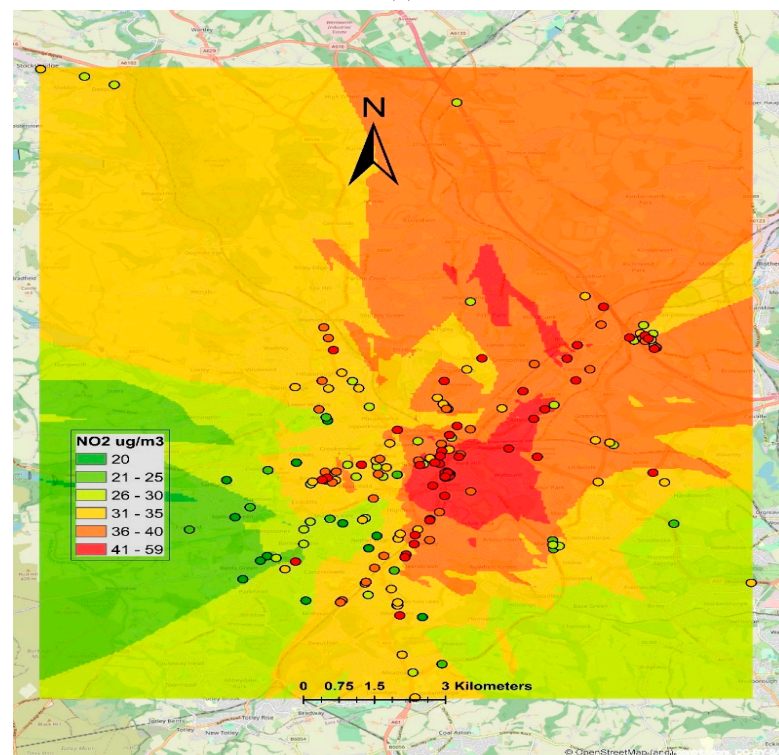
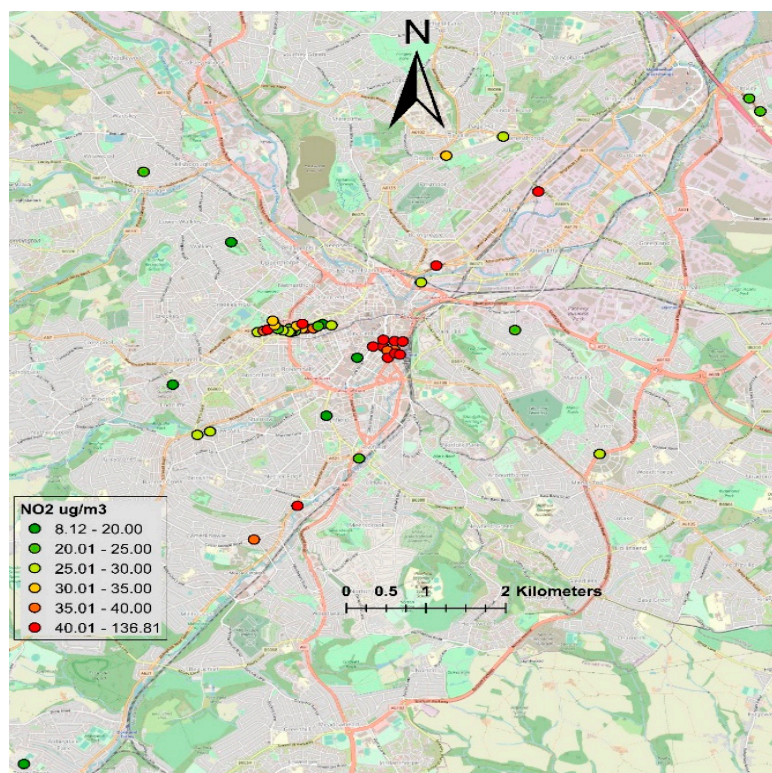(**b**)

Figure 4. Showing point and interpolated NO$_2$ levels from DT network: (**a**) NO$_2$ concentrations (μg/m^3) from DT, and (**b**) interpolated NO$_2$ concentrations (μg/m^3) using ordinary kriging.

Figure 5 shows NO$_2$ levels measured by LCS, ranging from 8.12 to 136.81 (μg/m^3). Exceedances of air quality standards are mainly shown in the city centre, where 10 Envirowatch E-MOTEs were installed. However, due to the low number of sensors com-

pared to DT, the interpolated maps are not as detailed as those produced by the DT. Envirowatch E-MOTEs installed in the city centre recorded relatively higher concentrations than the other parts of the city. Three Envirowatch E-MOTEs recorded particularly higher NO_2 concentrations: (a) outside Sheffield train station next to the taxi rank, E-MOTE 904 (136.81 μg/m^3), (b) Arundel Gate opposite to Genting Club, E-MOTE 732 (115.55 μg/m^3), and (c) Sheaf Street/Sheaf Square adjacent to the pedestrian crossing for Howard Street, E-MOTE 903 (107.17 μg/m^3). The reason for the higher concentrations is that these sites are very busy in terms of traffic flow and idling vehicles while stationary. The taxi stand (E-MOTE 904) is a good example, showing how idling vehicles contribute to air pollution in the city. E-MOTE 903 is installed next to a pedestrian crossing on a busy road. People coming out of the train station use the pedestrian crossing going towards the high street, Sheffield Hallam University and other parts of the city. The pedestrian crossing is regularly used, interrupting the traffic flow and causing congestion. When the lights turn red, road traffic stops but vehicle engines keep running. As soon as the lights turn green, all vehicles try to accelerate quickly. Therefore, idling of engine and sudden acceleration emits extra pollution, causing this location to be one of the most polluted sites. E-MOTE 732 is installed in a typical street canyon, where the road has tall buildings on both sides, hindering the dispersion of the pollutants emitted by the road traffic and causing the pollution levels to increase. The other sites in the city centre where air quality standards were exceeded are Paternoster Rows, Harmer Lane near Sheaf Street, Harmer Lane near the bus station, Arundel Gate near Surrey Street and Howard Street. Two E-MOTEs at the university campus that exceeded air quality limits were Regent Court and Broad Lane (near St. George's Terrace). In the outskirts of the city, air quality limits were exceeded at three sites where AQMesh pods were installed: Saville Street, Abbeydale Rd and Brightside Lane. At these sites, the main source of emission is road traffic. Therefore, road traffic is the main source of emissions causing violation of AQ standards in Sheffield.

(a)

Figure 5. *Cont.*
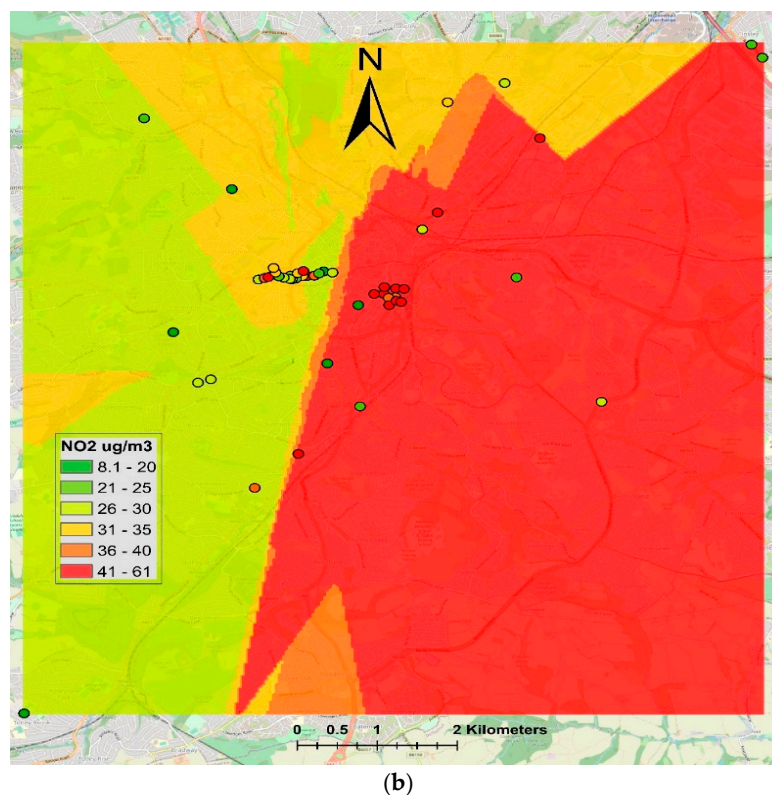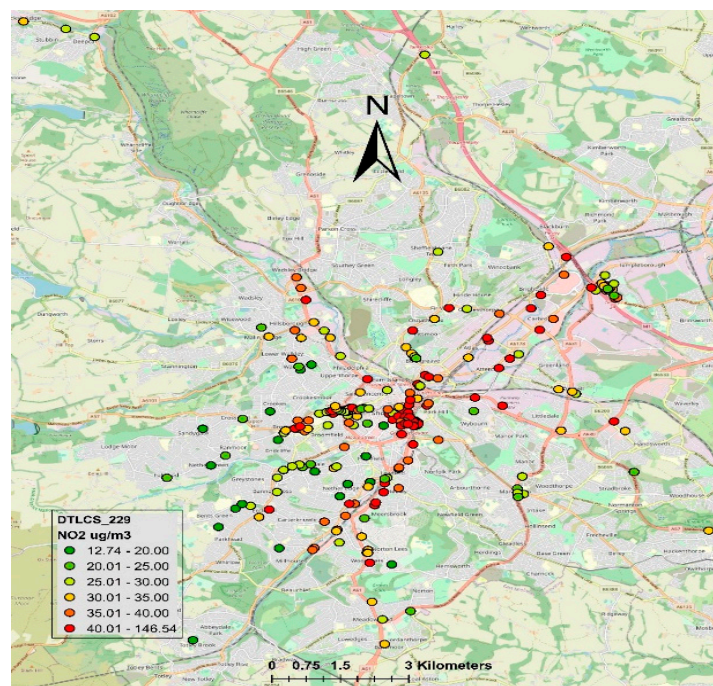
(**b**)

Figure 5. Showing point and interpolated NO$_2$ levels from LCS network: (**a**) NO$_2$ concentrations (μg/m^3) from LCS, (**b**) interpolated NO$_2$ concentrations (μg/m^3) using ordinary kriging.

Figure 6 combines both DT and LCS, showing a more detailed map of interpolated NO$_2$ concentrations (μg/m^3). Generally, it demonstrates the same pattern as shown in Figure 4. However, in comparison to LUR (Figure 3) and Airviro models (Figure 2), the interpolated maps are less precise and less detailed. Briggs et al. [10] compared the performance of LUR with spatial interpolation methods (e.g., kriging, Triangular Interpolation Network (TIN) contouring and trend surface analysis) and reported that LUR performed much better than the interpolation techniques. The reason probably was that in urban areas, spatial variability of air pollutants was more controlled by the local emission sources, such as road traffic, rather than a smoothly varying field, which was assumed by the interpolation methods.

3.2. Data Fusion—Fusing Model Estimations with Measured Concentrations

In this section, geostatistical universal kriging was used to fuse measured NO$_2$ concentrations with estimated NO$_2$ concentrations. NO$_2$ measured by DT, LCS and DTLCS are expressed as NO$_2$-DT, NO$_2$-LCS and NO$_2$-DTLCS and estimation of LUR and Airviro as NO$_2$-LUR and NO$_2$-Airviro, respectively.
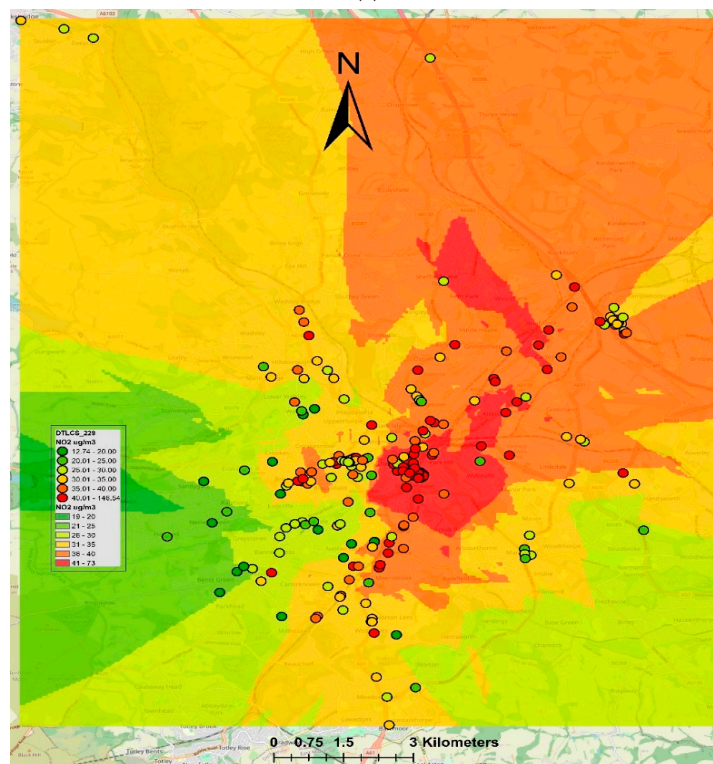
Figure 6. Showing point and interpolated NO_2 levels from both DT and LCS: (**a**) NO_2 concentrations ($\mu g/m^3$) from both 188 DT and LCS, and (**b**) interpolated NO_2 concentrations ($\mu g/m^3$) using ordinary kriging.

3.2.1. Fusion of NO_2-LCS with NO_2-Airviro and NO_2-LUR

Universal kriging was used to fuse NO_2-LCS with NO_2-Airviro and NO_2-LUR. Figure 7 presents the results of data fusion, where the fusion of NO_2-Airviro with measured NO_2 is presented in Figure 7a and the fusion of NO_2-LUR with measured NO_2 is presented

in Figure 7b. The resulting fused concentrations from the integration between NO_2-Airviro and NO_2-LCS (Airviro-LCS) ranged from 6.14 to 138.93 $\mu g/m^3$. The range of these values reflected the measured NO_2-LCS concentrations (ranging from 8.11 to 136.81 $\mu g/m^3$), whereas the spatial pattern followed the trend of NO_2-Airviro. On the other hand, the fusion of NO_2-LCS and NO_2-LUR (LUR-LCS) (Figure 7b) demonstrated a slightly different pattern. The NO_2 LUR-LCS ranged from 19.45 to 82.98 ($\mu g/m^3$), slightly overestimating lower values and underestimating the higher values. For model validation, the fused concentrations were compared with the measured concentrations using the testing dataset (25% randomly selected) applying various statistical metrics (Table 2). Overall, NO_2 LUR-LCS showed slightly better correlation (r, 0.96) and less error (RMSE, 9.09) than Airviro-LCS (r, 0.88 and RMSE, 18.16) when compared with measured concentrations. Overall, the fusion of Airviro-LCS slightly underestimated NO_2 concentrations, demonstrated by the negative value of MBE (−4.14).
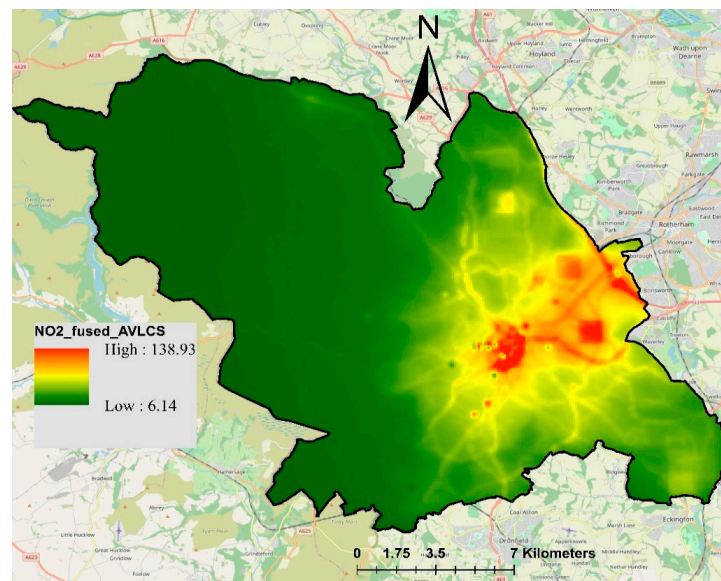
(a)
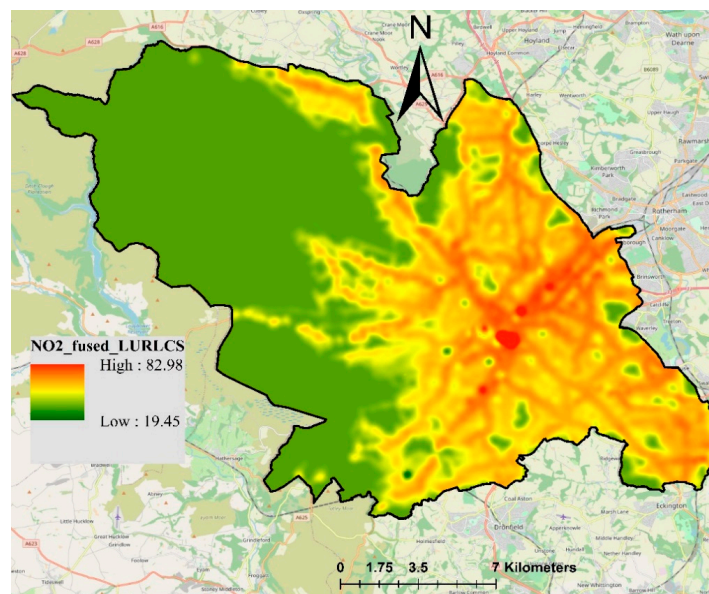
(b)

Figure 7. Resulting map of fused NO_2 concentrations ($\mu g/m^3$) using universal kriging techniques: (**a**) NO_2 Airviro-LCS; (**b**) NO_2 LUR-LCS.

Table 2. Showing the values of different statistical metrics calculated by comparing fused and measured NO_2 concentrations based on randomly selected testing dataset (train/test cross-validation). FAC2, MBE, MAE, RMSE and r stand for factor of two, mean biased error, mean absolute error, root mean squared error, and correlation coefficient.

Metrics	Airviro-LCS	LUR-LCS	Airviro-DT	LUR-DT	Airviro-DTLCS	LUR-DTLCS
FAC2	1	1	1	1	0.98	0.96
MBE	−4.14	1.44	1.56	1.40	1.08	2.24
MAE	12.79	7.99	5.81	5.29	8.20	3.73
RMSE	18.16	9.09	7.18	6.74	10.42	10.43
R	0.88	0.96	0.70	0.70	0.56	0.59

3.2.2. Fusion of NO_2-DT with NO_2-Airviro and NO_2-LUR

Maps produced by the fusion of NO_2-DT with NO_2-Airviro and NO_2-LUR are presented in Figure 8, where the fusion of Airviro-DT is shown in Figure 8a and the fusion of LUR-DT is shown Figure 8b. The fused NO_2 Airviro-DT ranged from 17.19 to 74.78 $\mu g/m^3$. NO_2-Airviro concentrations ranged from 0.69 to 110, whereas NO2-DT ranged from 13.58 to 91.75 $\mu g/m^3$. Airviro-DT showed higher concentrations in the city centre, east and northeast part of the city and relatively lower concentrations in the outskirts of the city, especially towards the west and northwest part of the city. Figure 8b shows NO_2 LUR-DT, which is the fusion between NO_2-LUR and NO_2-DT. Here, higher NO_2 LUR-DT are shown in the city centre, eastern and northeastern parts. However, some busy roads and hotspots are also highlighted in some other parts of the city. NO_2 LUR-DT ranged from 4.13 to 64.49 $\mu g/m^3$.

Statistical metrics used to compare measured concentrations with fused concentrations (Table 2) showed the same correlation coefficient for both LUR-DT and Airviro-DT (r, 0.70). The values of other metrics, e.g., RMSE and MAE, also demonstrated negligible differences. However, visually, LUR-DT produced more detailed maps and successfully highlighted higher pollution levels on several busy roads.

3.2.3. Fusion of NO_2-DTLCS with NO_2-Airviro and NO_2-LUR

Finally, the measured NO_2-DTLCS were fused with NO_2-Airviro and NO_2-LUR. The fused NO_2 concentrations are presented in Figure 9, where the fusion of Airviro-DTLCS is shown in Figure 9a and the fusion of LUR-DTLCS is shown in Figure 9b. The resulting maps shown in Figure 9 look similar to those presented in Figure 8 in terms of spatial coverage; however, actual values and their ranges are different. Fused Airviro-DTLCS ranged from 15.11 to 126.88, whereas LUR-DTLCS ranged from 19.45 to 82.98 $\mu g/m^3$. The measured NO_2-DTLCS ranged from 8.12 to 136.81 $\mu g/m^3$. Combining DT and LCS measurements did not improve the model performance compared to using only NO_2-DT. In contrast, the values of correlation coefficient slightly decreased to 0.56 and 0.59 for Airviro-DTLCS and LUR-DTLCS, respectively. Values of RMSE were 10.42 and 10.43 for Airviro-DTLCS and LUR-DTLCS, respectively (Table 2). This shows that increasing the number of sensors will not necessarily improve the output of the data fusion, especially if the sensors are not the same type.
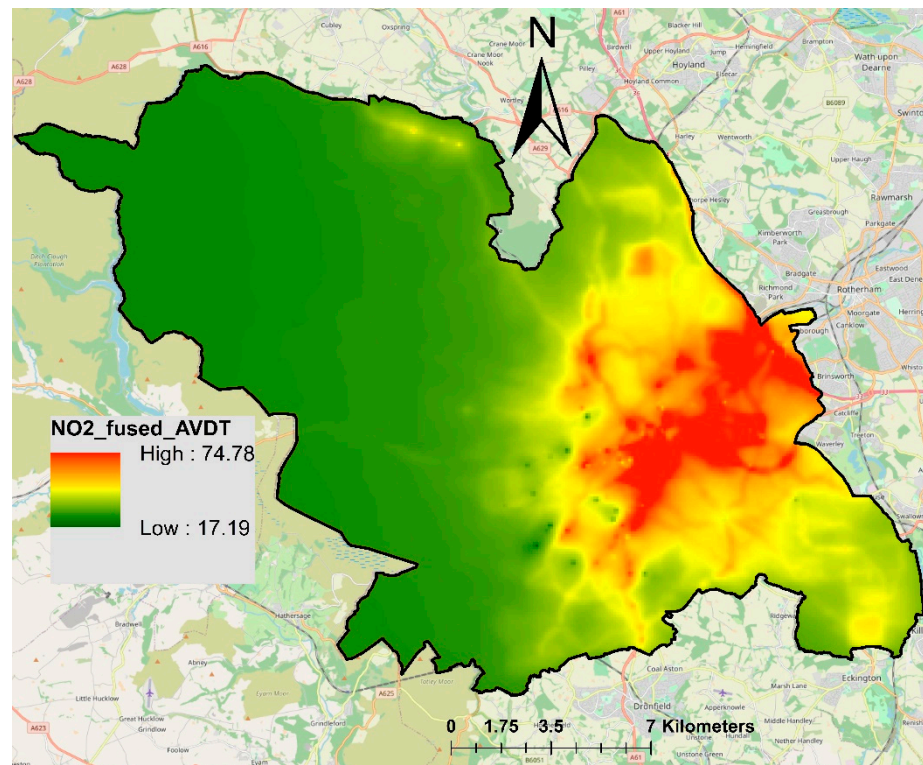
(a)
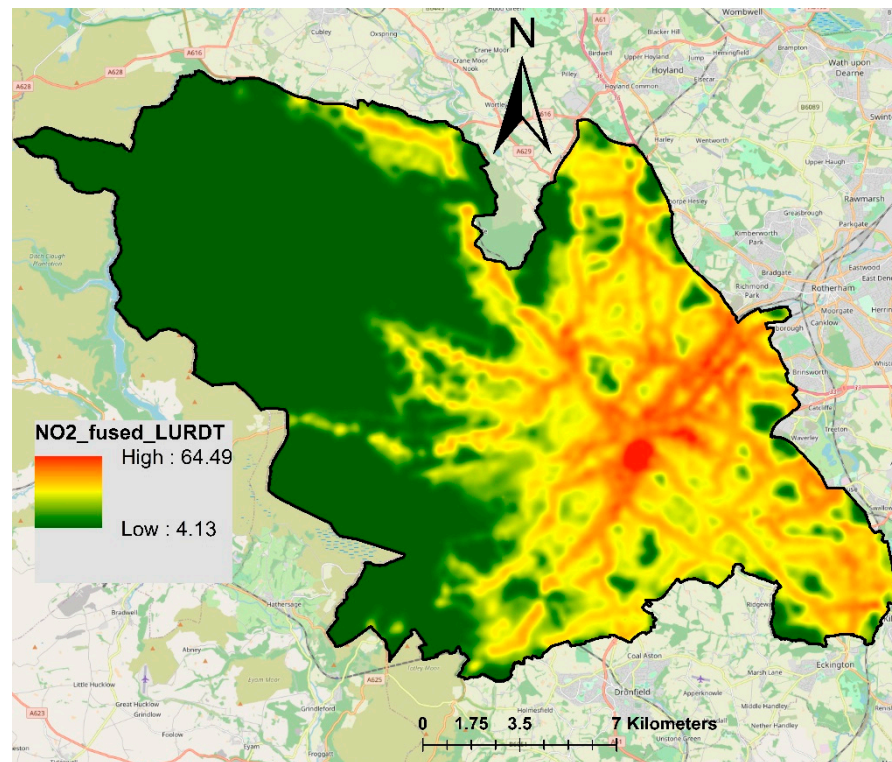
(b)

Figure 8. Resulting maps of fused NO$_2$ concentrations (μg/m^3) using universal kriging techniques: (**a**) NO$_2$ Airviro-DT; (**b**) NO$_2$ LUR-DT.
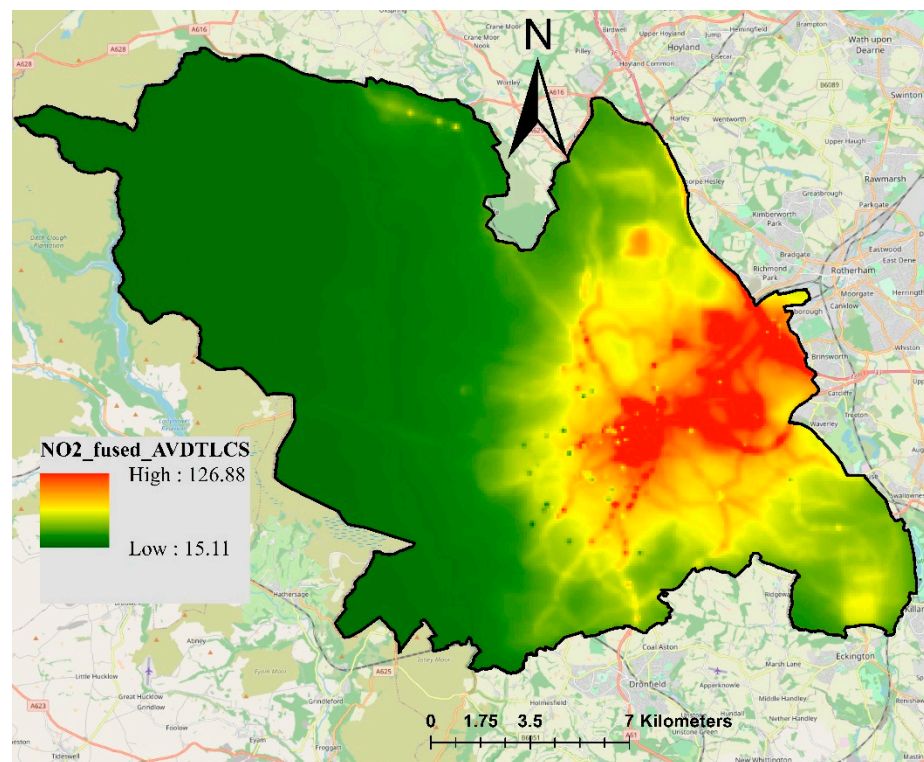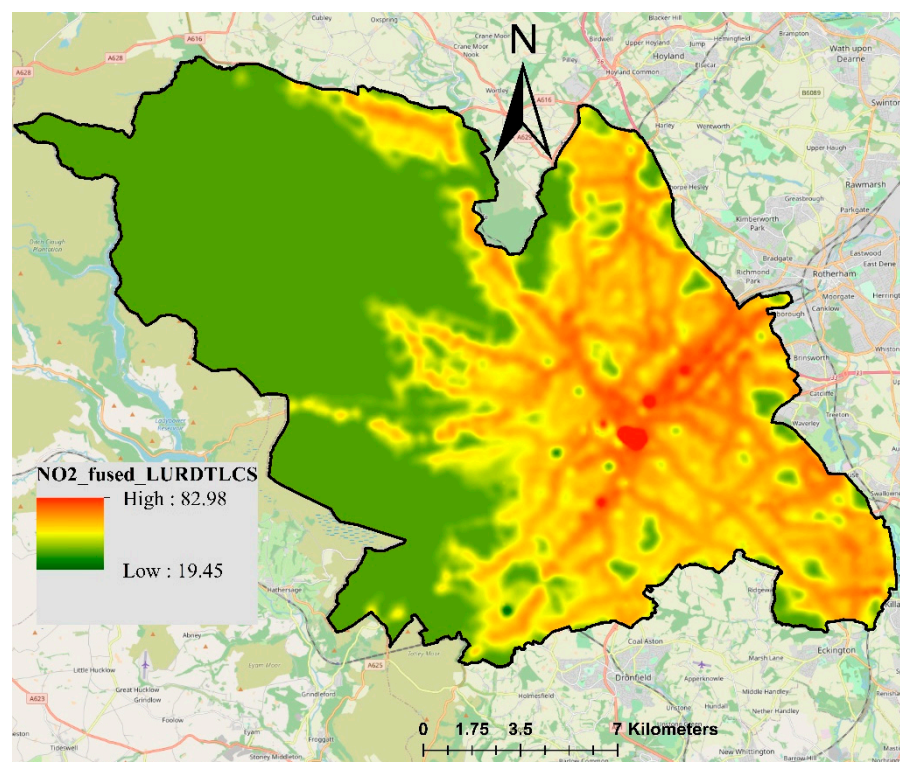
Figure 9. Resulting map of fused NO$_2$ concentrations (μg/m^3) using universal kriging techniques: (**a**) Airviro-DTLCS; (**b**) LUR-DTLCS.

The values of measured NO$_2$ concentrations are reflected in fused values, whereas the spatial trend is determined by the model values. The fused maps provided better coverage and more realistic concentrations than the interpolated maps using ordinary

kriging. Data fusion also improved the NO_2-Airvrio and NO_2-LUR maps, producing more realistic maps based on both measured and estimated concentrations. Overall, the fusion of LUR with measured concentrations produced better results than the Airviro model in terms of correlation coefficient, RMSE and MAE.

In this study, different monitoring and modelling approaches were used to produce high-resolution spatial maps of NO_2 concentrations in urban areas. Air quality monitoring is the more accurate source of data for assessing air pollutant levels. However, the air quality monitoring network cannot be dense enough to provide measured data for each spatial point in the whole city. Therefore, different modelling approaches (e.g., spatial interpolations, dispersion models and LUR models) are required to predict air quality information between monitoring stations. These models, in addition to measured data, use emission data, meteorology data, traffic characteristics, population data and land use characteristics. One of the issues with air quality modelling is its level of uncertainty, which is significantly higher than the measured data [27]. This is where data fusion techniques play their role by combining measured and modelled data in such a way to improve the spatiotemporal resolution of the measured data and accuracy of the modelled data.

Huang et al. [28] applied data fusion techniques to integrate measured and model estimation over North Carolina, USA. In contrast to this study, Huang et al. [28] analysed the levels of several air pollutants which were $PM_{2.5}$, CO, NOx, NO_2 and five particulate species (organic carbon, elemental carbon, and sulphate, nitrate and ammonium ions). They reported that the application of data fusion reduced biases in the model estimation. The correlation coefficient for the cross-validation test was 0.91 in Huang et al. [28], which was less than this study (r-value 0.96). Gressent et al. [29] analysed air quality data from low-cost sensors and integrated them with the estimation of ADMS-Urban in France. In contrast to this study, which uses annual NO_2 concentrations, Gressent et al. [29] used hourly data and estimated PM_{10} concentrations for 29 November 2018 from 7 a.m. to 7 p.m. They used external drift kriging, which is similar to universal kriging, and reduced the bias from 8% to 2% when considering LCS observations instead of the model alone. Schneider et al. [9] employed geostatistics methodology to fuse NO_2 concentrations obtained from a network of low-cost sensors (AQMesh) and EPISODE dispersion model. EPISODE is a 3-D Eulerian/Lagrangian dispersion model providing atmospheric air pollutant forecasts at urban and regional scales. For more details on the EPISODE model [30]. Schneider et al. [9] evaluated the geostatistics universal kriging methodology for fusing both measured and predicted data of NO_2 in Oslo, Norway during January 2016. Results showed that the fusing method was able to produce realistic hourly NO_2 concentrations, which inherited the spatial trend of the pollutant from the EPISODE model. Furthermore, fused data were compared to measured data from a reference instrument and results showed reasonably good resemblance between measured and fused data, with R^2 value of 0.89 and mean squared error of 14.3 μg/m^3. Their model showed slightly inferior performance in comparison to this study, with r-value 0.96 and RMSE 9.09. Furthermore, Schneider et al. [9] had used a shorter time-period of one month and fewer sensors as compared to this study, which used NO_2 data for a whole year from more sensors.

Most of the data fusion techniques mentioned above are applied on city scales. However, several researchers have also applied the data fusion approaches to air quality data on a country level [31] or global level [32]. Liang et al. [31] developed a data fusion method and compared the outputs with kriging-with-external-drift (KED) and the chemistry module from WRF-Chem (Weather Research and Forecast Model with Chemistry Module). KED is a type of universal kriging that takes into account the local trend of the variable (e.g., air pollutant concentrations) as well as external drift (a spatial trend) when minimising the variance of estimation [8]. Both KED and WRF-Chem were used to estimate daily $PM_{2.5}$ levels in 10-km grid cells in China during 2013. The estimated concentrations from both KED and WRF-Chem were then fused with measured observations. For fusion, a simple linear regression model was applied between the observed and estimated concentrations for both KED and chemistry models in turns. The regression coefficients obtained from the

regression model were used to adjust the predicted concentrations. The performance of the models was evaluated, and KED and regression data fusion methods showed better performance in terms of R^2 value of 0.95 and 0.94, respectively, as compared to the value of 0.51 for WARF-Chem model. Shaddick et al. [32], employing a Bayesian hierarchical modelling framework, estimated that 92% of the world's population lived in areas where air pollution levels exceeded the World Health Organization's air quality guidelines. However, the results of these investigations carried out on a country or global level are not comparable with studies conducted on a city level.

4. Conclusions

In this paper, different modelling and data fusion techniques were employed to analyse the spatial variability of NO_2 concentrations ($\mu g/m^3$) in the city of Sheffield. NO_2 was monitored by 188 DT, 41 low-cost sensors, 3 AURN and 5 SCC monitoring stations. The main difference between LCS and reference sensors is that LCS are cheaper, compact and their measurements are less reliable, whereas AURN and SCC use reference sensors which are much more expensive and reliable. However, the reference AQMN is sparse, having fewer AQMS, which are not enough for understanding the spatial variability of NO_2 in Sheffield. Therefore, the networks of LCS and DT were used for analysing the spatial variability of NO_2 concentrations and validating the models. Air quality standards were exceeded at several locations in Sheffield, particularly in the city centre and on some busy roads, where annual mean NO_2 levels were higher than 40 $\mu g/m^3$. The highest levels of NO_2 were recorded by the Envirowatch E-MOTE installed next to the Sheffield train station taxi rank (136.81 $\mu g/m^3$), followed by the Sheaf Street/Sheaf Square pedestrian crossing (115.56 $\mu g/m^3$) and Arundel Gate (107.17 $\mu g/m^3$).

Three modelling approaches were used to produce maps of NO_2 concentrations in Sheffield: (a) geostatistical kriging interpolation, (b) Airviro dispersion modelling, and (c) LUR based on the generalised additive model. Measured NO_2 concentrations were fused with the estimated concentrations using universal kriging, which is an advanced kriging technique that is employed for data having more than one correlated variable. Six sets of measured and estimated NO_2 data were fused: (i) Fusion of NO_2-Airviro with NO_2-LCS; (ii) Fusion of NO_2-Airviro with NO_2-DT; (iii) Fusion of NO_2-Airviro with NO_2-DTLCS; (iv) Fusion of NO_2-LUR with NO_2-LCS; (v) Fusion of NO_2-LUR with NO_2-DT; and (vi) Fusion of NO_2-LUR with NO_2-DTLCS. Fused NO_2 were compared with measured concentrations in terms of different statistical metrics including FAC2, r, RMSE, MAE and MBE. Maps produced by the fusion of NO_2-LCS and NO_2-LUR produced better results, with an r-value of 0.96, followed by the fusion of NO_2-Airviro with NO_2-LCS, with an r-value of 0.88. Fused maps developed by universal kriging provided better spatial coverage and similarity with measured concentrations than the ordinary kriging interpolation, Airviro and LUR models. Fused maps combining measured and estimated concentrations produced more realistic concentrations and provided better spatial coverage.

This study presents a geostatistical universal kriging approach for fusing measured and estimated NO_2 concentrations to improve our understanding of small-scale spatial variability in NO_2 concentrations in Sheffield. This approach adds value to both measured and estimated values: the measured concentrations are improved by predicting spatiotemporal gaps, whereas the modelled concentrations are improved by constraining them with observed data. The main findings of this study are: (a) The universal kriging approach was capable of estimating realistic NO_2 concentration maps from the fusion of measured and modelled concentrations. The fused NO_2 concentrations inherited spatial patterns of the pollutant from the model estimations and adjusted the modelled values using the measured concentrations. (b) A huge number of sensors are required to provide reasonable spatial coverage at a city level, which is too expensive. Spatial modelling (e.g., dispersion model and LUR model) and data fusion approaches can provide city-level maps by integrating pollutant concentrations measured by the AQMS with modelled concentrations. (c) According to Schneider et al. [9], the accuracy of the data fusion depends on the number

of sensors, their spatial distribution, their uncertainty and the accuracy of the estimated values to be fused with measured values. Here, we showed that in addition, the accuracy of the data fusion also depends on the uniformity of the sensors, meaning that using the same type of sensors can result in better accuracy. Increasing the number of sensors will not necessarily improve the model outputs, especially if sensors are not of the same type. For example, maps produced by the fusion of NO_2-LCS with NO_2-LUR (r-value 0.96) and NO_2-Airviro (r-value 0.88) produced better results than when both NO_2-DT and NO_2-LCS were used together and fused with NO_2-LUR or NO_2-Airviro, when the r-values decreased to 0.59 and 0.56, respectively.

The uniqueness of this study is that it uses estimated NO_2 concentrations from two sources—a dispersion model and a land use regression model—and measured NO_2 concentrations from three sources: diffusion tubes, reference sensors and low-cost sensors. The study applies geostatistical universal kriging for data fusion and produces high-resolution maps of NO_2 in Sheffield.

Limitations/weaknesses: (a) NO_2 diffusion tube data were downloaded from the Sheffield City Council website; we do not know which correction factors were applied before they were published online. (b) Low-cost sensors have their limitations and are not as accurate as reference sensors. The data from the low-cost sensors are postprocessed by the manufacturers with the aim of correcting cross-interferences as well as the effects of temperature and relative humidity. The AQMesh pods include an O_3-filtered NO_2 sensor from Alphasense, which is designed to reject O_3 and hence eliminate cross-sensitivity issues. However, none of these sensors was collocated with the reference sensor in the field; therefore, we could not develop and apply correction factors.

In the future, we aim to apply this approach to high-resolution spatiotemporal data (e.g., hourly data on city scale) to further improve spatiotemporal estimation of NO_2 concentrations. Furthermore, the data fusion work would be done in as near to real time as possible in the form of an app, so as to provide public health advice.

References

1. Public Health England. Guidance, Air pollution: Applying All Our Health. 2020. Available online: https://www.gov.uk/government/publications/air-pollution-applying-all-our-health/air-pollution-applying-all-our-health (accessed on 19 January 2021).
2. Fan, Z.; Pun, V.C.; Chen, X.C.; Hong, Q.; Tian, L.; Ho, S.S.H.; Lee, S.C.; Tse, L.A.; Ho, K.F. Personal exposure to fine particles (PM$_{2.5}$) and respiratory inflammation of common residents in Hong Kong. *Environ. Res.* **2018**, *164*, 24–31. [CrossRef]
3. WHO. Review of Evidence on Health Aspects of Air Pollution-REVIHAAP Project: Final Technical Report. *World Health Organziation Regional Office for Europe.* 2013. Available online: https://www.euro.who.int/__data/assets/pdf_file/0004/193108/REVIHAAP-Final-technical-report-final-version.pdf (accessed on 28 January 2021).
4. Landrigan, P.J. Air pollution and health. *Lancet Public Health* **2016**, *2*, 4–5. [CrossRef]

5. DEFRA. Improving Air Quality in the UK Tackling Nitrogen Dioxide in Our Towns and Cities, UK Overview Document, December 2015. Available online: https://www.gov.uk/government/uploads/system/uploads/attachment_data/file/486636/aq-plan-2015-overview-document.pdf (accessed on 9 April 2020).
6. Xie, X.; Semanjski, I.; Gautama, S.; Tsiligianni, E.; Deligiannis, N.; Rajan, R.T.; Pasveer, F.; Philips, W. A Review of Urban Air Pollution Monitoring and Exposure Assessment Methods. *ISPRS Int. J. Geo. inf.* **2017**, *6*, 389. [CrossRef]
7. Briggs, D.J. The Role of GIS: Coping with Space (And Time) in Air Pollution Exposure Assessment. *J. Toxicol. Environ. Health* **2005**, *68*, 1243–1261. [CrossRef]
8. Hengl, T.; Heuvelink, G.; Stein, A. *Comparison of Kriging with External Drift and Regression-Kriging*; ITC Technical note; International Institute for Geo-Information Science and Earth Observation (ITC): Enschede, The Netherlands, 2003.
9. Schneider, P.; Castell, N.; Vogt, M.; Dauge, F.R.; Lahoz, W.A.; Bartonova, A. Mapping urban air quality in near real-time using observations from lowcost sensors and model information. *Environ. Int.* **2017**, *106*, 234–247. [CrossRef] [PubMed]
10. Briggs, D.J.; de Hough, C.; Gulliver, J.; Wills, J.; Elliott, P.; Kingham, S.; Smallbone, K. A regression-based method for mapping traffic-related air pollution: Application and testing in four contrasting urban environments. *Sci. Total Environ.* **2000**, *253*, 151–167. [CrossRef]
11. Castanedo, F. A Review of Data Fusion Techniques. *Sci. World J.* **2013**, *2013*, 1–19. [CrossRef] [PubMed]
12. Munir, S.; Mayfield, M.; Coca, D.; Mihaylova, L.S. A nonlinear land-use regression approach for modelling NO_2 concentrations in urban areas—Using data from low-cost sensors and diffusion tubes. *Atmosphere* **2020**, *11*, 736. [CrossRef]
13. Munir, S.; Mayfield, M.; Coca, D.; Mihaylova, L.S.; Osammor, O. Analysis of air pollution in urban areas with Airviro dispersion model—A Case Study in the City of Sheffield, United Kingdom. *Atmosphere* **2020**, *11*, 285. [CrossRef]
14. Hiemstra, P. Automatic Interpolation Package. "Automap", Version 1.0-14, a Package for R Programming Language. 2015. Available online: https://cran.r-project.org/web/packages/automap/automap.pdf (accessed on 28 January 2021).
15. Briggs, D.J.; Collins, S.; Elliott, P.; Fischer, P.; Kingham, S.; Lebret, E.; Pryl, K.; van Reeuwijk, H.; Smallbone, K.; van der Veen, A. Mapping urban air pollution using GIS: A regression-based approach. *Int. J. Geogr. Inf. Sci.* **1997**, *11*, 699–718. [CrossRef]
16. Beelen, R.; Hoek, G.; Fischer, P.; van den Brandt, P.A.; Brunekreef, B. Estimated long-term outdoor air pollution concentrations in a cohort study. *Atmos. Environ.* **2007**, *41*, 1343–1358. [CrossRef]
17. Eeftens, M.; Beelen, R.; de Hoogh, K. Development of land use regression models for $PM_{2.5}$, $PM_{2.5}$ absorbance, PM_{10} and PM coarse in 20 European Study areas; results of the ESCAPE project. *Environ. Sci. Technol.* **2012**, *46*, 11195–11205. [CrossRef] [PubMed]
18. Hoek, G.; Beelen, R.; De Hoogh, K.; Vienneau, D.; Gulliver, J.; Fischer, P. A review of land-use regression models to assess spatial variation of outdoor air pollution. *Atmos. Environ.* **2008**, *42*, 7561–7578. [CrossRef]
19. Lee, J.-H.; Wu, C.-F.; Hoek, G.; De Hoogh, K.; Beelen, R.; Brunekreef, B.; Chan, C.-C. Land use regression models for estimating individual NO_x and NO_2 exposures in a metropolis with a high density of traffic roads and population. *Sci. Total. Environ.* **2014**, *472*, 1163–1171. [CrossRef]
20. Muttoo, S.; Ramsay, L.; Brunekreef, B.; Beelen, R.; Meliefste, K.; Naidoo, R.N. Land use regression modelling estimating nitrogen oxides exposure in industrial south Durban, South Africa. *Sci. Total Environ.* **2017**, *610–611*, 1439–1447. [CrossRef]
21. Rahman, M.M.; Yeganeh, B.; Clifford, S.; Knibbs, L.D.; Morawska, L. Development of a land use regression model for daily NO_2 and NOx concentrations in the Brisbane metropolitan area, Australia. *Environ. Modell. Softw.* **2017**, *95*, 168–179. [CrossRef]
22. Stedman, J.; Vincent, K.; Campbell, G.; Goodwin, J.; Downing, C. New high resolution maps of estimated background ambient NOx and NO_2 concentrations in the U.K. *Atmos. Environ.* **1997**, *31*, 3591–3602. [CrossRef]
23. Ryan, P.H.; LeMasters, G.K.; Biswas, P.; Levin, L.; Hu, S.; Lindsey, M.; Bernstein, D.I.; Lockey, J.; Villareal, M.; Hershey, G.K.K.; et al. A comparison of proximity and land use regression traffic exposure models and wheezing in infants. *Environ. Health Perspect.* **2007**, *115*, 278–284. [CrossRef]
24. Ryan, P.H.; LeMasters, G.K. A review of land-use regressionmodels for characterizing intraurban air pollution exposure. *Inhal. Toxicol.* **2007**, *19* (Suppl. 1), 127–133. [CrossRef]
25. Goovaerts, P. *Geostatistics for Natural Resources Evaluation*; Applied Geostatistics Series; Oxford University Press: Oxford, UK, 1997; ISBN 0-19-511538-4.
26. R Core Team. *R: A Language and Environment for Statistical Computing*; R Foundation for Statistical Computing: Vienna, Austria, 2019; Available online: https://www.R-project.org/ (accessed on 28 January 2021).
27. Denby, B.; Garcia, V.; Holland, D.M.; Hogrege, C. Integration of air quality modeling and monitoring data for enhanced health exposure assessment. *Air Waste Manag. Assoc.* **2009**, *10*, 46–49.
28. Huang, R.; Zhai, X.; Ivey, C.E.; Friberg, M.D.; Hu, X. Using Air Quality Model-Data Fusion Methods for Developing Air Pollutant Exposure Fields and Comparison with Satellite AOD-Derived Fields: Application over North Carolina, USA. In *Air Pollution Modeling and Its Application XXV*; Mensink, C., Kallos, G., Eds.; Springer Proceedings in Complexity Book Series; Springer: Cham, Switzerland, 2018. [CrossRef]
29. Gressent, A.; Malherbe, L.; Colette, A.; Rollin, H.; Scimia, R. Data fusion for air quality mapping using low-cost sensor observations: Feasibility and added-value. *Environ. Int.* **2020**, *143*, 105965. [CrossRef] [PubMed]
30. Slordal, L.H.; Walker, S.E.; Solberg, S.S. *The Urban Air Dispersion Model EPISODE Applied in AirQUIS 2003—Technical Description*; NILU—Norwegian Institute for Air Research: Kjeller, Norway, 2003.

31. Liang, F.; Gao, M.; Xiao, Q.; Carmichael, G.R.; Pan, X.; Liu, Y. Evaluation of a data fusion approach to estimate daily PM2.5 levels in North China. *Environ. Res.* **2017**, *158*, 54–60. [CrossRef] [PubMed]

32. Shaddick, G.; Thomas, M.L.; Green, A.; Brauer, M.; van-Donkelaar, A.; Burnett, R. Data integration model for air quality: A hierarchical approach to the global estimation of exposures to ambient air pollution. *J. R. Stat. Soc. Ser. Appl. Stat.* **2018**, *67*, 231–253. [CrossRef]